Supporting Information

High Redox Potential Chromophores for Visible Light-Driven Water Oxidation at Low pH

Lei Wang,[§] *David W. Shaffer,*[†] *Gerald F. Manbeck,*[⊥] *Dmitry E. Polyansky,*[⊥] *Javier J. Concepcion*[⊥*]

[§]Department of Materials Science and Chemical Engineering, Stony Brook University, Stony Brook, New York 11794, United States

[⊥]Chemistry Division, Brookhaven National Laboratory, Upton, New York 11973, United States

Corresponding author email address: jconcepc@bnl.gov

Experimental Methods

Materials. High-purity water was obtained by passing house-distilled water through a Millipore Milli-Q Synthesis A-10 system. Perchloric and nitric acids (70%, Aldrich, 99.999% trace metals grade) were used to prepare 0.1 M HNO_3 or $HClO_4$. 4-bromo-2,2′-bipyridine and 5-bromo-2,2′-bipyridine were purchased from Ark Pharm, Inc. All other reagents and solvents were purchased from commercial sources and used as received.

Physical Methods. Nuclear magnetic resonance (NMR) spectra were recorded on a Bruker Avance III 400 spectrometer. ^{1}H NMR spectra were referenced to the residual protio impurities of the solvent.[1] All chemical shifts (δ) are reported in ppm. High resolution Electrospray ionization mass spectrometry (HR-ESI-MS) was performed with a Thermo Scientific™ Q Exactive™ Mass Spectrometer using methanol as the eluent. Elemental analyses (EA) were performed by Robertson Microlit Laboratories (Ledgewood, NY, USA). Reported pH values were measured on a Fisher Scientific Accumet Micro glass electrode after calibration with standard buffer solutions. Electronic absorption spectra were recorded with a UV-visible Agilent 8453 diode-array spectrophotometer and were corrected for the background spectrum of the solvent. Fluorescence spectroscopy were measured with a PTI QuantaMaster system with the FelixGX software. Electrochemical measurements were performed with a CH Instruments CH-760E bipotentiostat at ambient temperature (21-24 °C) in a single compartment cell with a 3.0 mm glassy carbon disc working electrode, platinum wire counter electrode, and Ag/AgCl (3 M NaCl) reference electrode. The reference electrode was calibrated to the Ru(III/II) couple of an internal $[Ru(bpy)_3][NO_3]_2$ standard at 1.26 V *vs* NHE.[2] Emission lifetimes ($\boldsymbol{\tau_0}$) were recorded using optically dilute samples in quartz cuvettes that were sealed with septa and deoxygenated by bubbling with argon. Samples were excited with a continuously tunable OPO (Opotek) pumped by a Q-switched Nd: YAG at 355 nm. The instrument was operated at 5 Hz with 2.5–3 mJ per pulse and ~6 ns pulse width. Emission was probed at 90° to the laser pulse and focused on an ISA monochromator. The signal was detected using a Hamamatsu R955 PMT, digitized with an oscilloscope, and fit to single exponential decay kinetics. Each reported lifetime is an average of 32 kinetic traces.

Pressure measurements were conducted in a 4 mL cuvette with constant stirring at room temperature (22 ± 1 °C). The cuvette was sealed with a septum that was connected to a Honeywell pressure sensor (SDX30G2-A or SDX05G2-A). The pressure changes of the headspace were recorded with a real-time data acquisition system (InstruNet i555). The 454 nm monochromatic

light source was an LED driven by an American Reliance Inc. (AMREL) programmable DC power supply (applied current: 5A). For a typical measurement, 20 μM Ru(bda)(isq)$_2$, 200 μM chromophore and 1 M (or 1.58M) $Na_2S_2O_8$ were dissolved in 0.1 M $HClO_4$ in the cuvette then a septum was inserted and the pressure inside the flask was released through a needle until the pressure reading reached zero (vs. atmospheric). After removing the needle, the pressure sensor was connected, the light was turned on, and the software was triggered to record the changes of headspace pressure with time. The rate and turnover frequency (TOF) were obtained from the maximum slope of the oxygen evolution plot. The turnover numbers (TONs) were calculated from the total amount of oxygen generated.

The molar extinction coefficients, ε ($M^{-1}cm^{-1}$), were calculated by the Beer-Lambert Law: $\varepsilon = \frac{A}{cl}$, where the concentration, c, is measured in mol dm^{-3} (M^{-1}) and the cell path length, l, in cm. The emission intensity was measured by using 20 μ M chromophores in 0.1 M $HClO_4$.

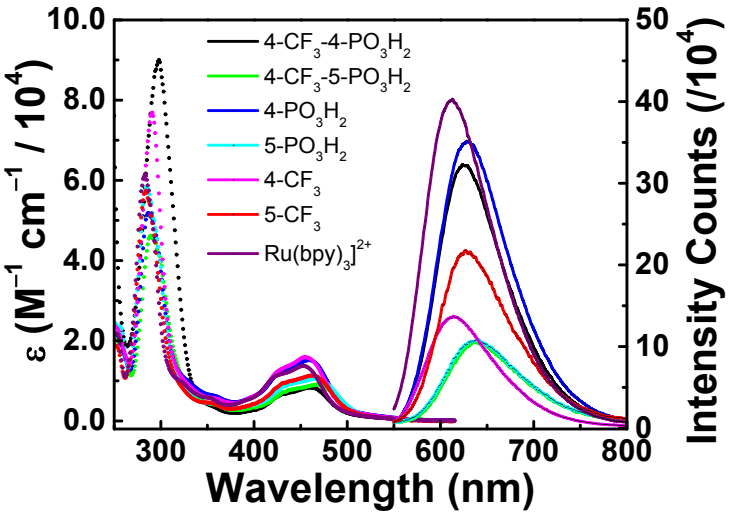

Figure S1. Absorption and emission spectra for the chromophores in 0.1 M $HClO_4$.

The photophysical properties of the chromophores are summarized in Table S1. λ_{00} was taken as the wavelength value at which the tangent of the high energy side of the emission crosses the wavelength-axis. Other parameters were calculated as follows:

$$E\ (cm^{-1}) = 10^7 / \lambda\ (\text{nm}) \quad \text{(eq. S1)}$$

$$E\ (\text{eV}) = E(cm^{-1}) / 8065 \quad \text{(eq. S2)}$$

$$E_{1/2}\ (\text{Ru}^{\text{III/II*}}) = E_{1/2} - E_{00}(eV)/F \quad \text{(eq. S3) with F = 1 eV/V}$$

Table S1. Photophysical properties for the chromophores $[Ru(L)_3]^{2+}$.[a]

L	$E_{1/2}$ (V vs NHE)	$\lambda_{max, MLCT}$ (nm)	$\lambda_{max, ex}$ (nm)	$\lambda_{max, em}$ (nm)	$\lambda_{00, em}$ [b] (nm)	E_{00} (eV)	$E_{1/2}$ ($Ru^{III/II*}$) (eV)
4-CF_3-4'-PO_3H_2-bpy	1.602	461	467	624	594	2.087	-0.485
4-CF_3-5'-PO_3H_2-bpy	1.600	468	468	640	611	2.029	-0.429
4-PO_3H_2-bpy	1.342	458	467	628	593	2.091	-0.749
5-PO_3H_2-bpy	1.340	467	468	640	608	2.039	-0.699
4-CF_3-bpy	1.512	455	467	617	585	2.120	-0.608
5-CF_3-bpy	1.536	464	467	630	600	2.067	-0.531
bpy	1.260	454	466	611	584	2.123	-0.863

[a] 20 μM chromophores in 0.1M $HClO_4$ solution at room temperature. [b] $\lambda_{00, em}$ was obtained by the crossover point of tangent line of emission spectrum with wavelength.

Table S2 summarizes the calculated photophysical parameters. K_{sv} is calculated from emission quenching data as a function of the concentration of persulfate, which follows the Stern-Volmer relationship:

$$\frac{I_0}{I} = k_{sv}[S_2O_8{}^{2-}] + 1 \quad \text{(eq. S4)}$$

where $K_{sv} = \tau_0 k_q$. The quantum yield was calculated according to Lakowicz's method in *Principles of fluorescence spectroscopy*.[3] As shown in equation S5, Φ is the quantum yield, *Int* is the area under the emission peak (on a wavelength scale), *A* is absorbance at the excitation wavelength, and η is the refractive index of the solvent.

$$\Phi_p = \Phi_{ref} \times \frac{Int_p}{Int_{ref}} \times \frac{(1-10^{-A_{ref}})}{(1-10^{-A_p})} \times \frac{n_p^2}{n_{ref}^2} \quad \text{(eq. S5)}$$

Considering the similar absorbance value and the same solvent (0.1 M $HClO_4$) in the experiment, the above equation can be simplified as equation S6:

$$\Phi_p = \Phi_{ref} \times \frac{Int_p}{Int_{ref}} \quad \text{(eq. S6)}$$

where Φ_{ref} is 0.042 according to Van Houten and Watts' work[4]. Then k_{nr} can be calculated by using equation S7 and S8 below:

$$k_r \tau_0 = \Phi_p \quad \text{(eq. S7)}$$

$$\tau_0^{-1} = k_r + k_{nr} \quad \text{(eq. S8)}$$

Table S2. Photophysical parameters for the chromophores $[Ru(L)_3]^{2+}$ based on Table S1.

L	E_{00} (cm^{-1})	k_{SV} (M^{-1})	τ_0 (ns)	Φp	$10^{-4}•k_r$ (s^{-1})	$10^{-6}•k_{nr}$ (s^{-1})
4-CF_3-4′-PO_3H_2-bpy	16835	6.8	667	0.0334	5.01	1.45
4-CF_3-5′ -PO_3H_2-bpy	16366	2.2	222	0.0123	5.54	4.45
4-PO_3H_2-bpy	16863	64	534	0.0379	7.10	1.8
5-PO_3H_2-bpy	16447	11	147	0.0128	8.71	6.72
4-CF_3-bpy	17094	344	731	0.0141	1.93	1.35
5-CF_3-bpy	16667	17	258	0.0238	9.22	3.78
bpy	17123	929	580	0.042	7.24	1.65

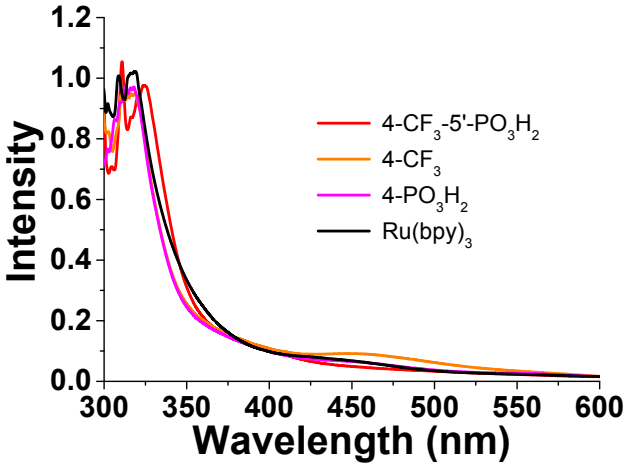

Figure S2. UV-vis spectra of chromophores after photochemical water oxidation experiments.

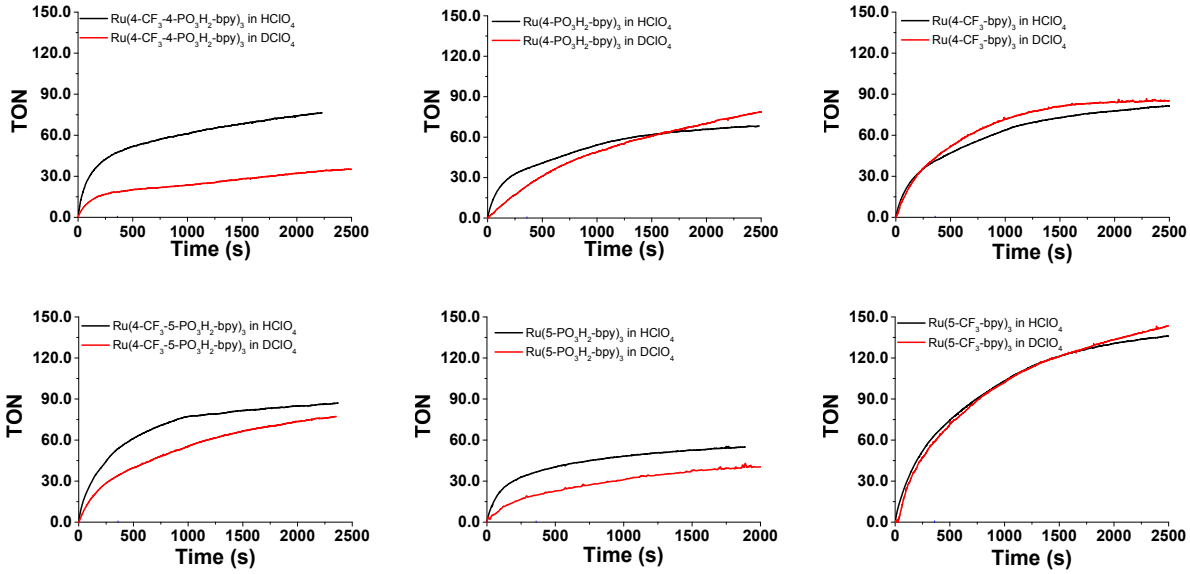

Figure S3. TON as a function of time for the chromophores in 0.1M $HClO_4$ and $DClO_4$ at room temperature.

The pK_a of $[(bpy)_2Ru(5\text{-}PO(OH)_2\text{-}bpy)]Cl_2$ ($E_{1/2}$ = 1.26 vs NHE) was determined by spectroelectrochemistry at various pH values, with an applied potential of 1.56 V vs NHE. Ru^{II} shows an absorption peak at 288 nm while Ru^{III} shows an absorption peak at 315 nm. Monitoring the UV-vis spectra, once the absorption at 315 nm stopped increasing with applied potential, Ru^{III} generation was considered complete.

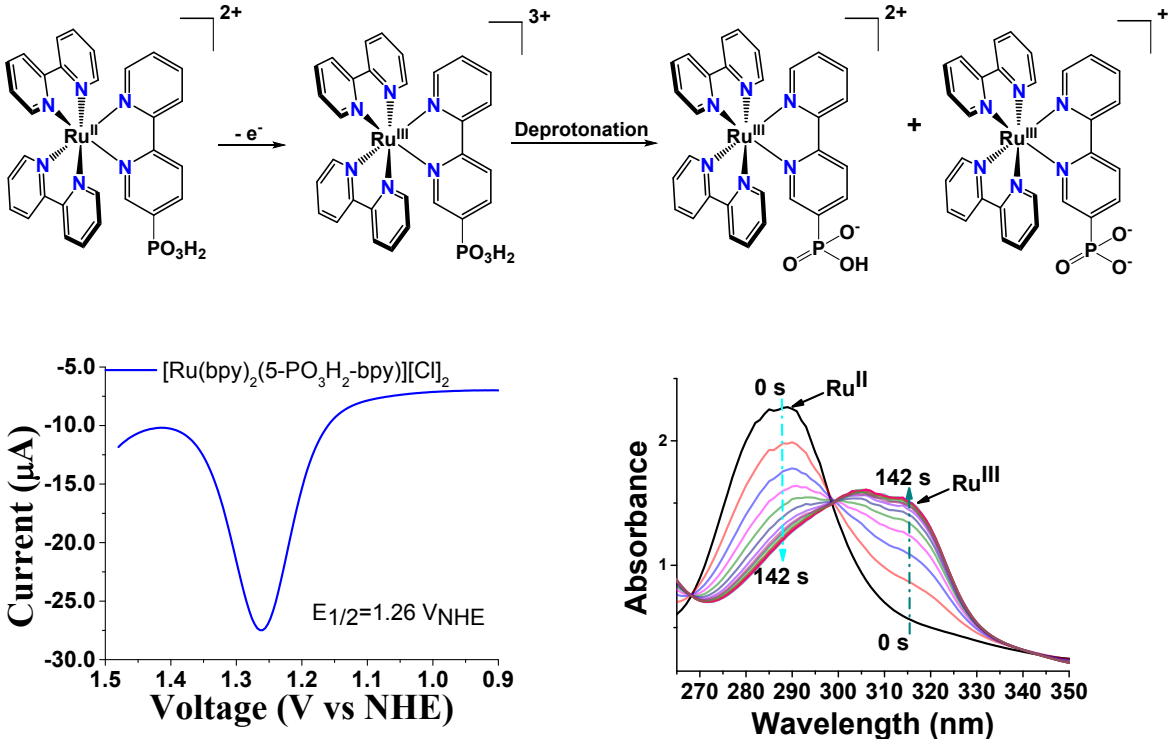

Figure S4. (*left*) Square wave voltammograms and (right) spectra recorded during spectroelectrochemical experiment of 1mM $[(bpy)_2Ru(5\text{-}PO(OH)_2\text{-}bpy)]Cl_2$ in 0.1M $HClO_4$.

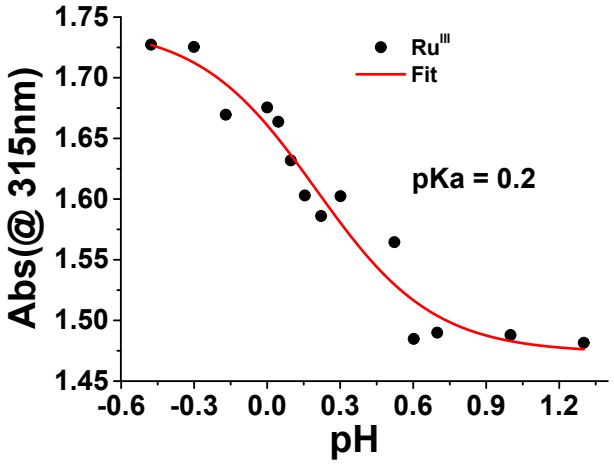

Figure S5. Absorbance vs pH traces at 315nm for $[(bpy)_2Ru(5\text{-}PO_3H_2\text{-}bpy)]Cl_2$, applied potential: 1.56V vs NHE.

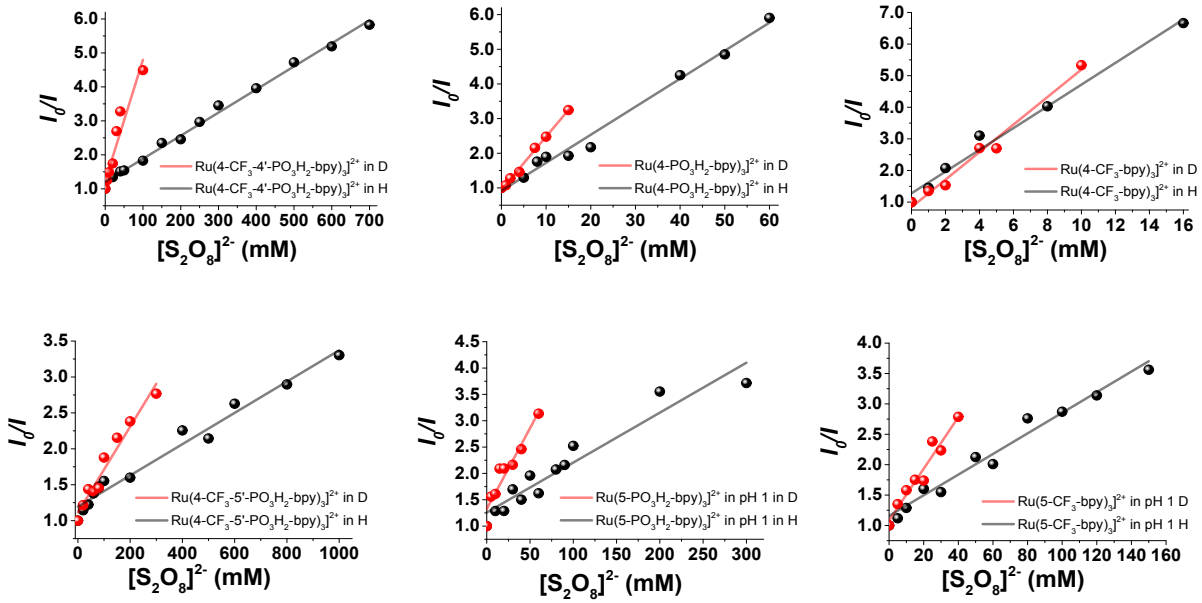

Figure S6. Stern Volmer Plots for chromophores in 0.1 M $HClO_4$ and $DClO_4$ at room temperature.

Table S3. K_{sv}, τ_o, and k_q data for the chromophores $[Ru(L)_3]^{2+}$ in 0.1 M $HClO_4$ and $DClO_4$.

L	Solvent	K_{SV} (M^{-1})	$K_{SV,H}$ / $K_{SV,D}$	τ_o (ns)	$\tau_{0,H}/\tau_{0,D}$	k_q ($M^{-1}s^{-1}$)	$k_{q,H}/k_{q,D}$
4-CF_3-4-PO_3H_2-bpy	$HClO_4$	6.8	0.19	667	0.58	$1.0 * 10^7$	0.32
	$DClO_4$	35.6		1150		$3.1 * 10^7$	
4-CF_3-5-PO_3H_2-bpy	$HClO_4$	2.2	0.36	222	0.58	$9.9 * 10^6$	0.62
	$DClO_4$	6.0		383		$1.6 * 10^7$	
4-PO_3H_2-bpy	$HClO_4$	64	0.42	534	0.52	$1.2 * 10^8$	0.80
	$DClO_4$	153		1028		$1.5 * 10^8$	
5-PO_3H_2-bpy	$HClO_4$	11	0.36	147	0.53	$7.5 * 10^7$	0.68
	$DClO_4$	30.7		276		$1.1 * 10^8$	
4-CF_3-bpy	$HClO_4$	344	0.79	731	0.66	$4.7 * 10^8$	1.20
	$DClO_4$	435		1107		$3.9 * 10^8$	
5-CF_3-bpy	$HClO_4$	17	0.40	258	0.55	$6.6 * 10^7$	0.73
	$DClO_4$	42.5		469		$9.1 * 10^7$	

To show the effect of $Na_2S_2O_8$ concentration on water oxidation activity, the theoretical concentration of $Na_2S_2O_8$ to quench 90% of the emission was calculated as shown in Table S4. In $HClO_4$, it requires 4 M $Na_2S_2O_8$ to quench 90% of the emission for 4-CF_3-5-PO_3H_2-bpy while in our experiments, 1.58 M was used limited by the solubility of $Na_2S_2O_8$.

Table S4. Calculated required $Na_2S_2O_8$ concentration (M) to quench 90% emission of the chromophores $[Ru(L)_3]^{2+}$ in 0.1M $HClO_4$ and $DClO_4$. [a]

L	$HClO_4$	$DClO_4$
4-CF_3-4-PO_3H_2-bpy	1.29	0.245
4-CF_3-5-PO_3H_2-bpy	4	1.44
4-PO_3H_2-bpy	0.14	0.059
5-PO_3H_2-bpy	0.80	0.29
4-CF_3-bpy	0.03	0.024
5-CF_3-bpy	0.52	0.21
bpy	0.01	--

[a] Calculations are based on the results in Figure S6.

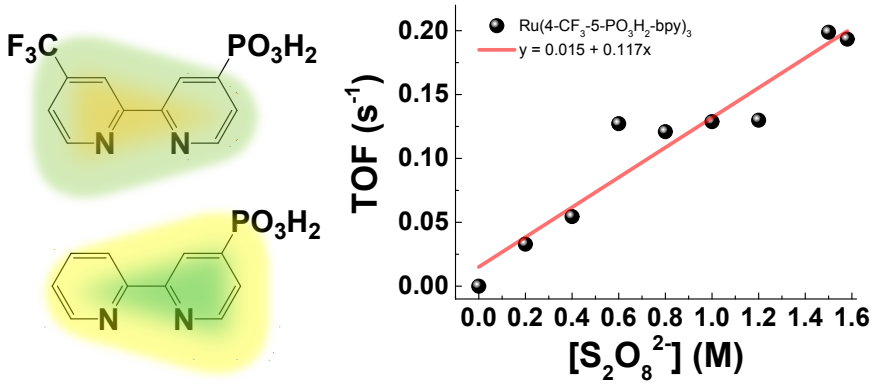

Figure S7. Electron density distribution (*left*). TOF calibration of $Ru(4\text{-}CF_3\text{-}5\text{-}PO_3H_2\text{-}bpy)_3]^{2+}$ in 0.1M $HClO_4$ (*right*).

To gain further understanding of the mechanism for photochemical water oxidation catalysis, the kinetics of [Ru(bda)(isq)$_2$]-catalyzed photochemical water oxidation were studied using pressure measurements. [Ru(bda)(isq)$_2$] displayed two different kinetic regimes, with rate laws depending on the catalyst concentration: zero order in catalyst at higher concentrations and first order in catalyst at lower concentrations. This kinetic behavior is the same as chemical water oxidation of Ru(bda)(isq)$_2$ catalysts in solution with Ce^{IV} as the oxidant.[5] The rate laws for these two regimes are represented by equations S9 and S10, respectively. The catalyst concentration at which the rate-determining step changes, represented by the red "X " in Figure S8 , is the value of $[Ru]_X$ for which the two rate laws are equal (eq. S9 = eq. S10), as shown in eq. S11. [Ru]x is 21.7 μM, while in chemical water oxidation with Ce(IV) is 9.2 μM.

$$\frac{rate}{[Ru]} = \text{TOF} = \frac{k[Ru]^2}{[Ru]} = k_1[\text{Ru}] \quad \text{(eq. S9)}$$

$$\frac{rate}{[Ru]} = \text{TOF} = \frac{k \times [Ru] \times [Ox]}{[Ru]} = k_0[O_X] \quad \text{(eq. S10)}$$

$$[\text{Ru}]_X = \frac{k_0[Ox]}{k_1} \quad \text{(eq. S11)}$$

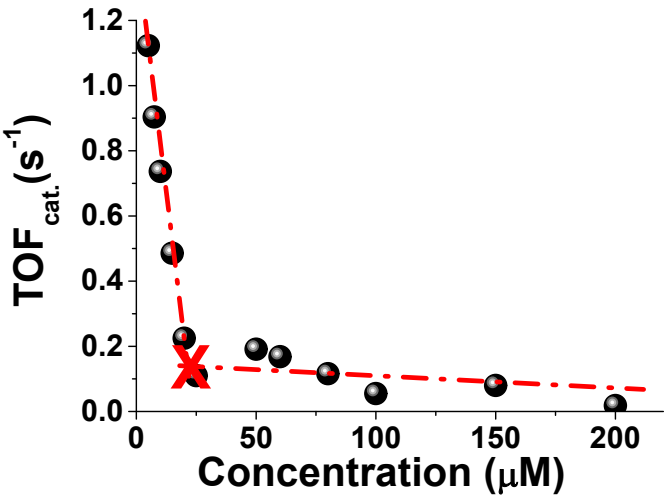

Figure S8. Ru(bda)(isq)$_2$ TOF as a function of catalyst concentration in 0.1 M $HClO_4$. Condition: 200 μM Chromophore $[Ru(5\text{-}PO_3H_2\text{-}bpy)_3]^{2+}$, 1.5M $Na_2S_2O_8$ at 25 °C.

Table S5. KIEs of chromophores $[Ru(L)_3]^{2+}$ in 0.1 M Nitric Acid (pH 1).

L	Solvent	TON	TOF_{max} (s^{-1})	KIE
4-CF_3-4-PO_3H_2-bpy	HNO_3	135	0.245	1.40
	DNO_3	100	0.175	
4-CF_3-5-PO_3H_2-bpy	HNO_3	110	0.143	1.09
	DNO_3	110	0.131	
4-PO_3H_2-bpy	HNO_3	140	0.245	1.81
	DNO_3	120	0.135	
5-PO_3H_2-bpy	HNO_3	130	0.220	2.44
	DNO_3	140	0.090	
4-CF_3-bpy	HNO_3	120	0.205	0.95
	DNO_3	130	0.215	
5-CF_3-bpy	HNO_3	170	0.188	0.87
	DNO_3	160	0.215	

[a] KIE was obtained from photochemical water oxidation experiments. Condition: 200 μM chromophore; 20 μM catalyst, Ru(bda)(isq)$_2$; 1 M or 1.5 M $Na_2S_2O_8$ at 25 °C.

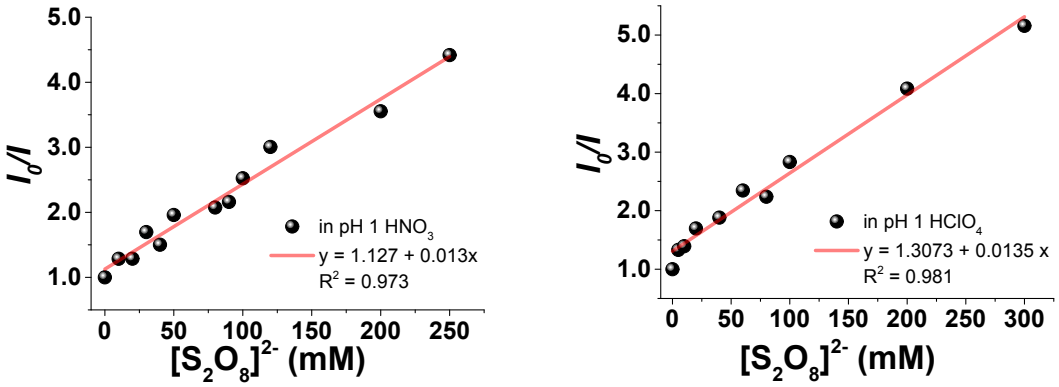

Figure S9. Stern Volmer Plot for $[Ru(5\text{-}PO_3H_2\text{-}bpy)_3]^{2+}$ in (*left*) 0.1M $HClO_4$ and (*right*) 0.1M HNO_3 at room temperature.

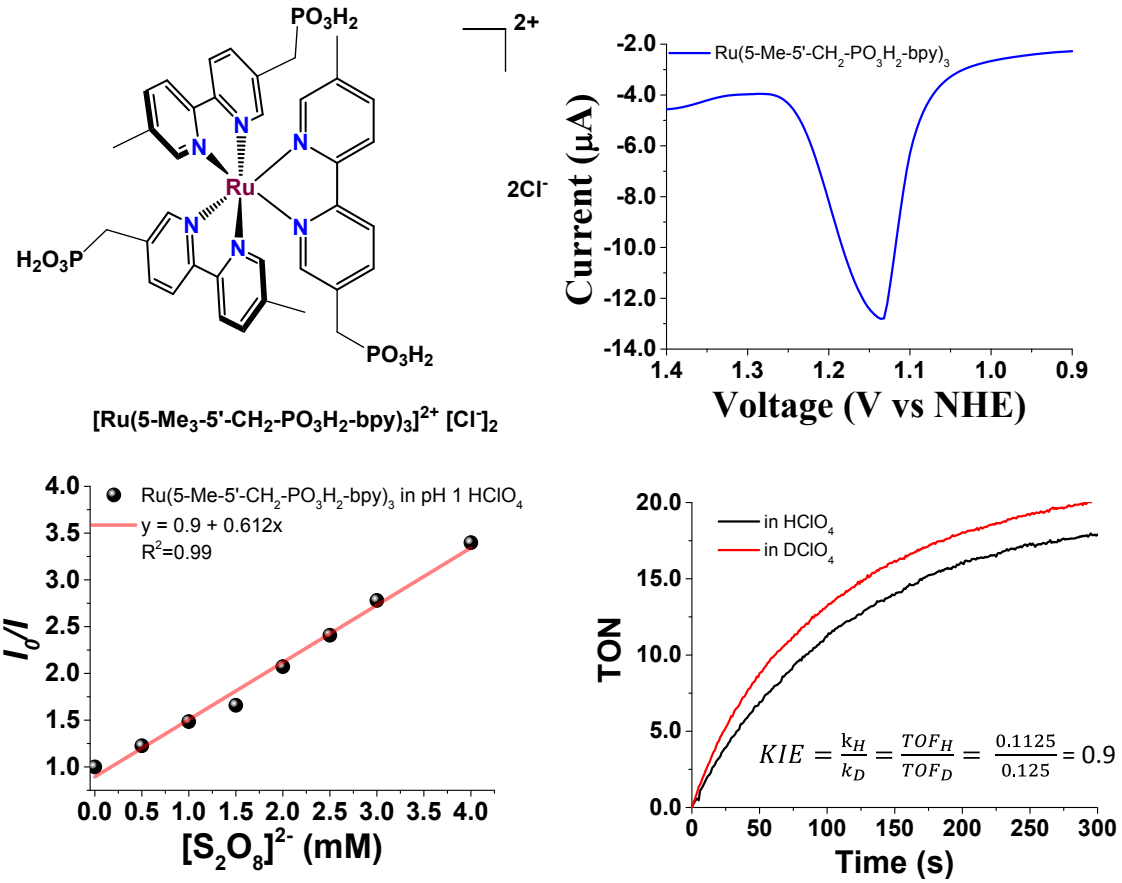

Figure S10. [Ru(5-Me-5'-CH_2-PO_3H_2-bpy)$_3$]$^{2+}$[Cl^-]$_2$ properties: (*top left*) molecular structure; (*top right*) square wave voltammograms; (*bottom left*) Stern Volmer Plot; (*bottom right*) TON changing with time.

Synthetic Procedures

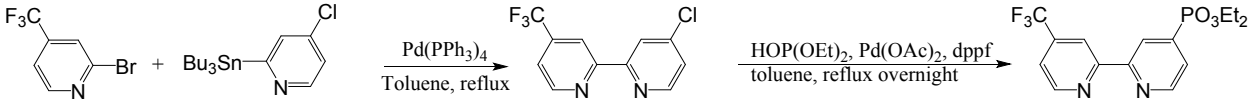

Figure S11. Synthesis of diethyl (4'-(trifluoromethyl)-[2,2'-bipyridin]-4-yl)phosphonate ligand.

Synthesis of 4-chloro-4′-(trifluoromethyl)-2, 2′-bipyridine. An oven-dried round-bottomed flask was charged with tetrakis(triphenylphosphine)palladium(0) (220 mg, 0.19 mmol) and placed under an argon atmosphere. 2-bromo-4-(trifluoromethyl) pyridine (430 mg, 1.91 mmol), 4-chloro-2-(tributylstannyl) pyridine (1 g, 2.48 mmol) and 60 mL anhydrous toluene were added. The reaction mixture was degassed with argon for 15 min and slowly warmed up to 120 ^{o}C and refluxed under argon overnight. After cooling, the solid material was separated by filtration. The filtrate was taken to dryness by rotatory evaporation and a dark brown oil was obtained. The crude product was dissolved in 100 mL dichloromethane and extracted with 6 M HCl (30 mL × 3). The combined aqueous phase was neutralized with 25% ammonium hydroxide to pH ~8. The white solid product that precipitated was collected by vacuum filtration, washed with 10% NH_4OH and then water. The product was dried under vacuum to provide 440 mg of a white solid in 89% yield. ^{1}H NMR (400 MHz, $CDCl_3$): δ 8.83 (d, J = 5.0 Hz, 1H), 8.66 (s, 1H), 8.58 (d, J = 5.2 Hz, 1H), 8.47 (d, J = 1.5 Hz, 1H), 7.54 (d, J = 4.7 Hz, 1H), 7.35 (dd, J = 5.2, 1.8 Hz, 1H).

Synthesis of diethyl (4'-(trifluoromethyl)-[2,2'-bipyridin]-4-yl)phosphonate. An oven-dried round-bottomed flask was charged with 4-chloro-4′-(trifluoromethyl)-2,2'-bipyridine (350 mg, 1.356 mmol), palladium(II) acetate (30 mg, 0.136 mmol), bis(diphenylphosphino)ferrocene (150 mg, 0.272 mmol) and placed under an argon atmosphere. Diethyl phosphite (420 uL, 3.26 mmol), triethylamine (460 uL, 3.26 mmol) and 50 mL anhydrous toluene were added. The reaction mixture was degassed with argon for 15 min and slowly warmed up to 120 ^{o}C then refluxed under argon overnight. After cooling, solids were separated by filtration, the filtrate was taken to dryness by rotatory evaporation, and a dark brown oil was obtained. The crude product was purified by column chromatography on silica (100% dichloromethane then 98% dichloromethane with 2% methanol) to provide the title compound as yellow oil (325 mg, 0.9 mmol). Yield: 67 %. ^{1}H NMR (400 MHz, $CDCl_3$): δ 8.88 – 8.76 (m, 3H), 8.67 (s, 1H), 7.73 (dd, J = 13.0, 4.3 Hz, 1H), 7.53 (d, J = 4.1 Hz, 1H), 4.25 – 4.11 (m, 4H), 1.35 (t, J = 7.0 Hz, 6H).

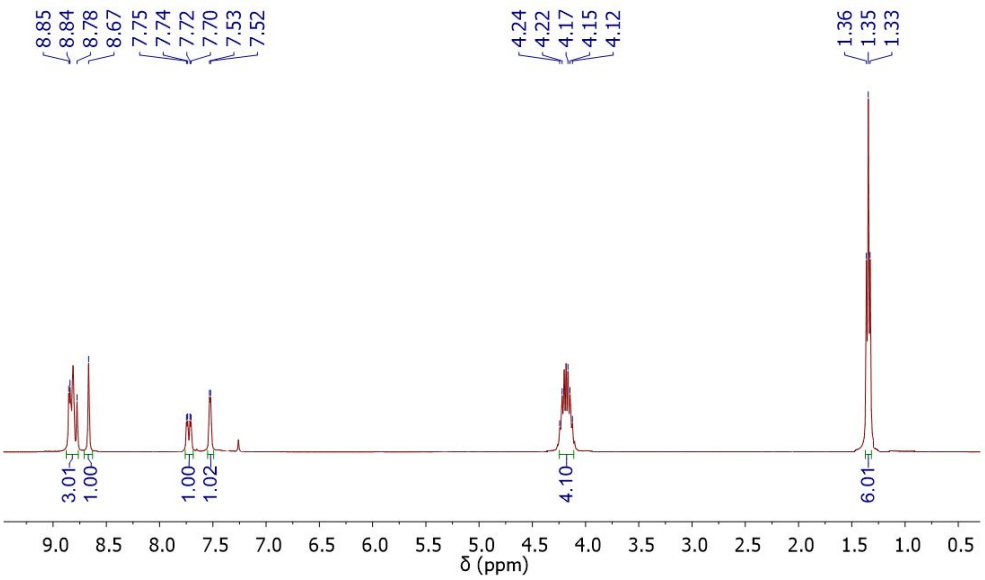

Figure S12. ^{1}H NMR spectrum for 4′-CF_3-4-PO_3Et_2-bpy in $CDCl_3$.

Synthesis of diethyl (4′-(trifluoromethyl)-[2,2′-bipyridin]-5-yl)phosphonate. Diethyl (4′-(trifluoromethyl)-[2,2′-bipyridin]-5-yl)phosphonate was synthesized using the same procedure used for diethyl (4′-(trifluoromethyl)-[2,2′-bipyridin]-4-yl)phosphonate but using 5-chloro-2-(tributylstannyl) pyridine (1 g, mmol) and 5-chloro-4′-(trifluoromethyl)-2,2′-bipyridine (365 mg, 1.02 mmol). After chromatography (100% dichloromethane then 98% dichloromethane with 2% methanol), some diethyl phosphite remained; however, it does not affect the next step, and the material was used without further purification. Yield: 75 %. ^{1}H NMR (400 MHz, $CDCl_3$): δ 9.04 (d, J = 6.1 Hz, 1H), 8.87 (d, J = 5.0 Hz, 1H), 8.74 (s, 1H), 8.55 (dd, J = 7.9, 2.8 Hz, 1H), 8.29 – 8.21 (m, 1H), 7.57 (d, J = 4.8 Hz, 1H), 4.26 – 4.07 (m, 4H), 1.36 (t, J = 7.1 Hz, 6H).

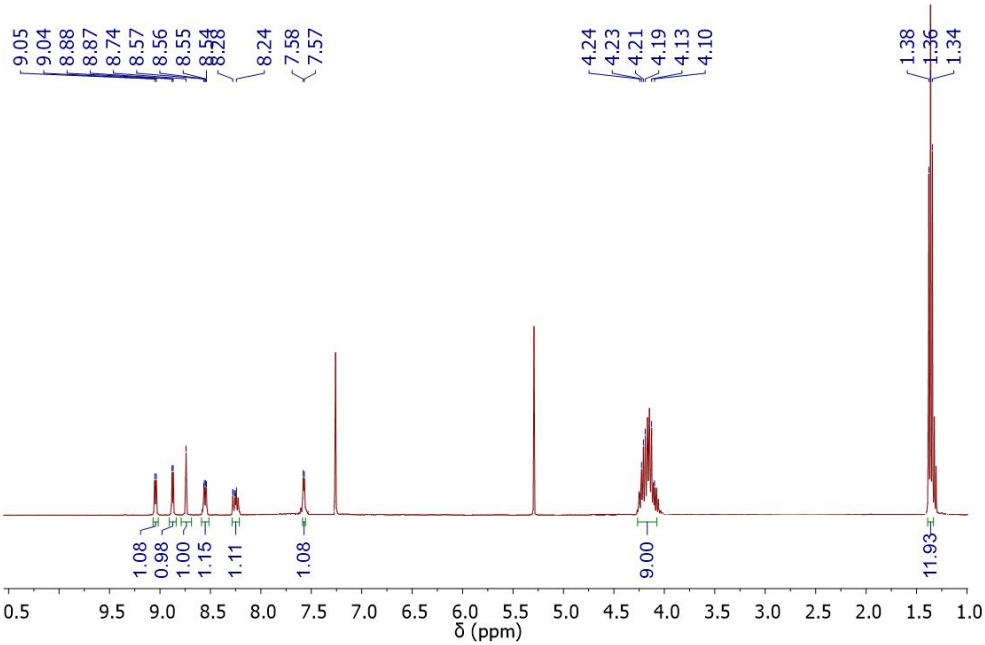

Figure S13. ^{1}H NMR spectrum for 4′-CF_3-5-PO_3Et_2-bpy in $CDCl_3$.

Synthesis of diethyl [2,2′-bipyridin]-4-ylphosphonate. diethyl [2,2′-bipyridin]-4-ylphosphonate was synthesized by a procedure similar to diethyl (4'-(trifluoromethyl)-[2,2'-bipyridin]-4-yl)phosphonate using 4-chloro-2,2′-bipyridine (290 mg, 1.53 mmol). After chromatography (100% dichloromethane then 98% dichloromethane with 2% methanol), some diethyl phosphite remained, and the material was used without further purification. Yield: 88 %. ^{1}H NMR (400 MHz, $CDCl_3$): δ 9.03 (d, J = 6.0 Hz, 1H), 8.71 (d, J = 4.6 Hz, 1H), 8.56 – 8.42 (m, 2H), 8.21 (ddd, J = 12.8, 8.1, 1.7 Hz, 1H), 7.85 (t, J = 7.0 Hz, 1H), 7.39 – 7.33 (m, 1H), 4.16 (td, J = 14.3, 7.1 Hz, 8H), 1.36 (td, J = 7.1, 2.7 Hz, 11H), 1.24 (t, J = 7.0 Hz, 3H).

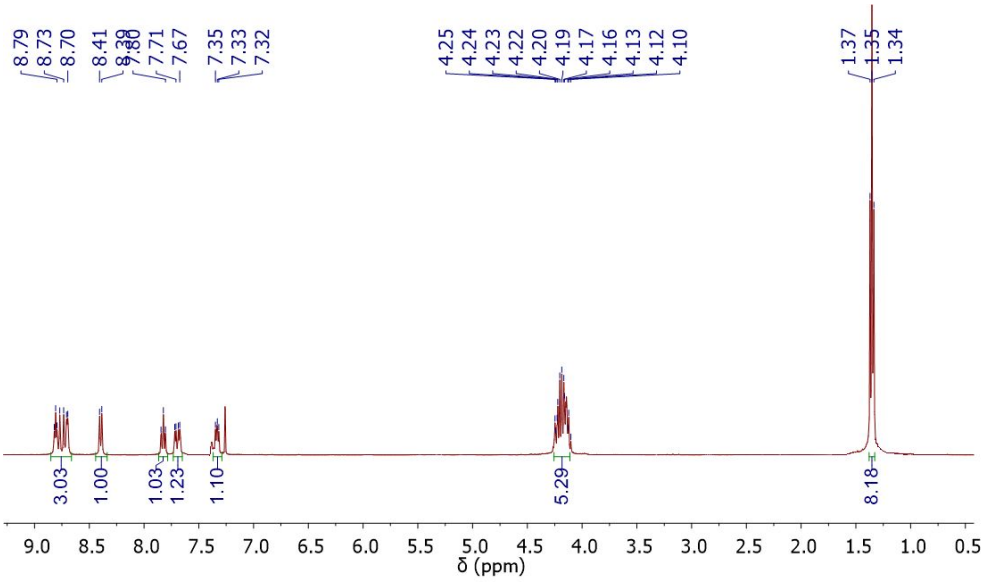

Figure S14. ^{1}H NMR spectrum for 4-PO_3Et_2-bpy in $CDCl_3$.

Synthesis of diethyl [2,2′-bipyridin]-5-ylphosphonate. [2,2′-bipyridin]-5-ylphosphonate was synthesized by a procedure similar to [2,2'-bipyridin]-4-ylphosphonate using 5-chloro-2,2′-bipyridine (330 mg, 1.73 mmol) in place of 4-chloro-2,2′-bipyridine. After chromatography (100% dichloromethane then 98% dichloromethane with 2% methanol), some diethyl phosphite remained, and the material was used without further purification. Yield: 93 %. ^{1}H NMR (400 MHz, $CDCl_3$): δ 9.03 (d, J = 6.0 Hz, 1H), 8.71 (d, J = 4.6 Hz, 1H), 8.56 – 8.42 (m, 2H), 8.21 (ddd, J = 12.8, 8.1, 1.7 Hz, 1H), 7.85 (t, J = 7.0 Hz, 1H), 7.39 – 7.33 (m, 1H), 4.16 (td, J = 14.3, 7.1 Hz, 8H), 1.36 (td, J = 7.1, 2.7 Hz, 11H), 1.24 (t, J = 7.0 Hz, 3H).

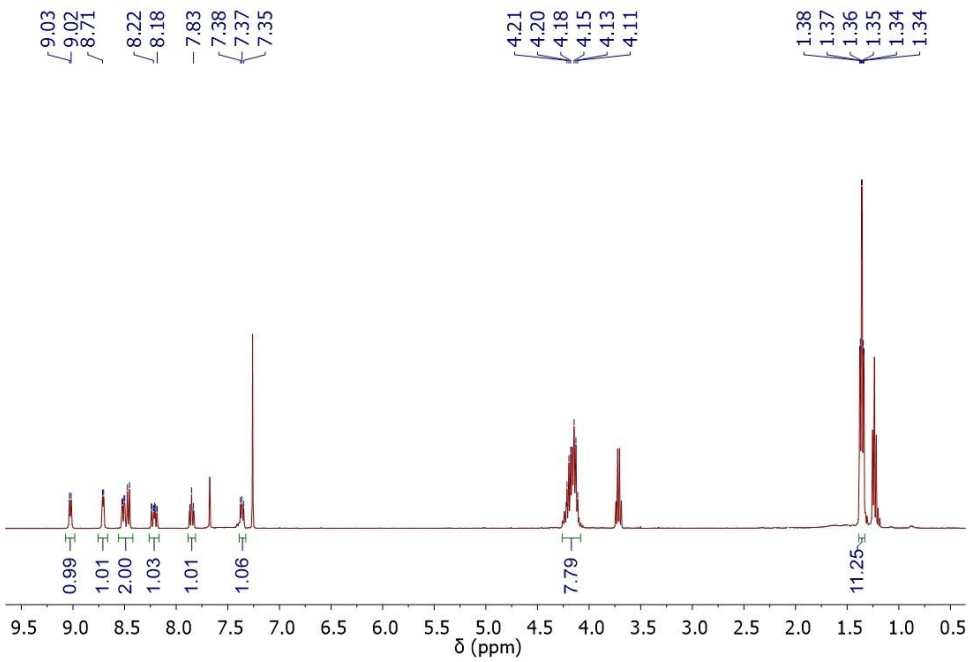

Figure S15. ^{1}H NMR spectrum for 5-PO_3Et_2-bpy in $CDCl_3$.

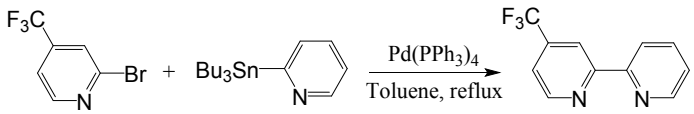

Figure S16. Synthesis of 4-(trifluoromethyl)-2,2′-bipyridine ligand.

Synthesis of 4-(trifluoromethyl)-2,2′-bipyridine. 4-(trifluoromethyl)-2,2′-bipyridine was synthesized by a procedure similar to 5′-chloro-4-(trifluoromethyl)-2,2′-bipyridine except that 2-(tributylstannyl) pyridine (1.06 mg, 2.8mmol) was used in place of 5-chloro-2-(tributylstannyl) pyridine. Yield: 80%. ^{1}H NMR (400 MHz, $CDCl_3$): δ 8.84 (d, J = 5.0 Hz, 1H), 8.71 (dd, J = 7.1, 3.0 Hz, 2H), 8.44 (d, J = 8.0 Hz, 1H), 7.85 (td, J = 7.8, 1.7 Hz, 1H), 7.56 – 7.47 (m, 1H), 7.36 (ddd, J = 7.5, 4.8, 1.0 Hz, 1H).

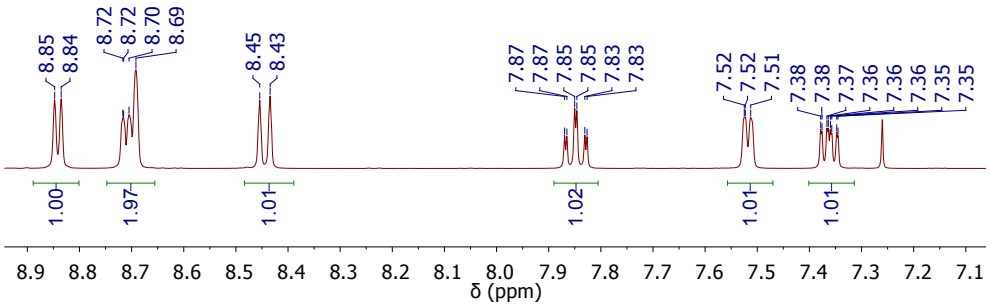

Figure S17. ^{1}H NMR spectrum for 4-CF_3-bpy in $CDCl_3$.

Synthesis of 5-(trifluoromethyl)-2,2′-bipyridine. 5-(trifluoromethyl)-2,2'-bipyridine was synthesized by a procedure similar to 4-(trifluoromethyl)-2,2′-bipyridine except that 2-bromo-5-(trifluoromethyl) pyridine (500 mg, 2.22 mmol) was used in place of 2-bromo-4-(trifluoromethyl) pyridine. Yield: 80%. ^{1}H NMR (400 MHz, $CDCl_3$): δ 8.92 (s, 1H), 8.70 (s, 1H), 8.64 – 8.35 (m, 2H), 8.04 (s, 1H), 7.84 (s, 1H), 7.36 (s, 1H).

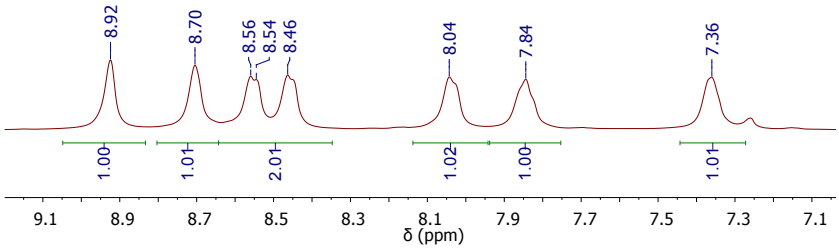

Figure S18. ^{1}H NMR spectrum for 5-CF_3-bpy in $CDCl_3$.

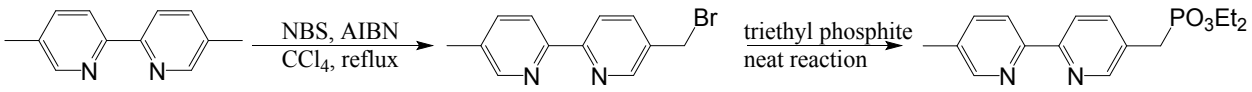

Figure S19. Synthesis of diethyl ((5′-methyl-[2,2'-bipyridin]-5-yl)methyl)phosphonate ligand.

Synthesis of diethyl ((5′-methyl-[2,2′-bipyridin]-5-yl)methyl)phosphonate. A round-bottomed flask was charged with 5,5′-dimethyl-2,2′-bipyridine (3.1 g, 16.8 mmol), NBS (3 g, 16.8 mmol), and AIBN (140 mg, 5% eq.) then placed under an argon atmosphere. 75 mL anhydrous carbon tetrachloride was added. The reaction mixture was degassed with argon for 10 min then refluxed at 77 °C for 17 hours. The mixture was filtered while hot, and the filtrate was stored in a refrigerator for 2 days to precipitate out any dibromo derivative which was separated by filtration. After rotary evaporation of the filtrate, the 5-(bromomethyl)-5′-methyl-2,2′-bipyridine was obtained as a white solid (yield: 67%). 5-(bromomethyl)-5′-methyl-2,2'-bipyridine (4.78 mmol) was then reacted with triethyl phosphite (28 mmol) at 90 °C under Ar for 5 hours. The crude product was purified by chromatography on silica (100% dichloromethane then 98% dichloromethane with 2% methanol) to provide 2.95 g (9.23 mmol) of the title compound as a yellow oil. Yield: 82%. ^{1}H NMR (400 MHz, $CDCl_3$): δ 8.52 (s, 1H), 8.46 (s, 1H), 8.28 (d, J = 8.2 Hz, 1H), 8.22 (d, J = 8.1 Hz, 1H), 7.77 – 7.71 (m, 1H), 7.59 (d, J = 8.1 Hz, 1H), 4.02 (dd, J = 15.2, 7.1 Hz, 4H), 3.16 (d, J = 21.7 Hz, 2H), 2.36 (s, 3H), 1.24 (t, J = 7.0 Hz, 6H).

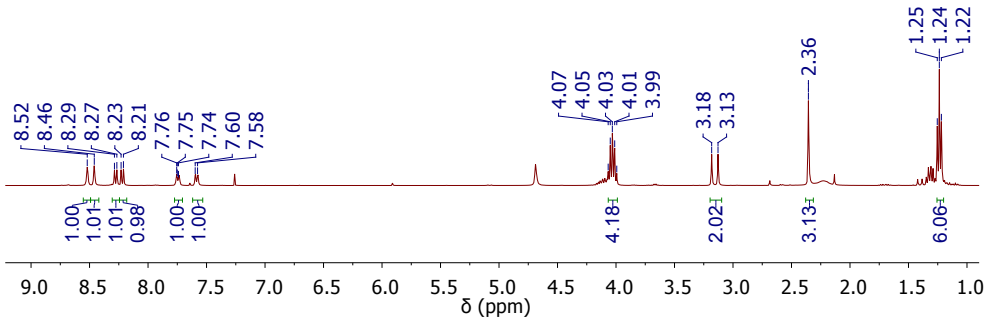

Figure S20. ^{1}H NMR spectrum for 5-Me-5′-CH_2-PO_3Et_2-bpy in $CDCl_3$.

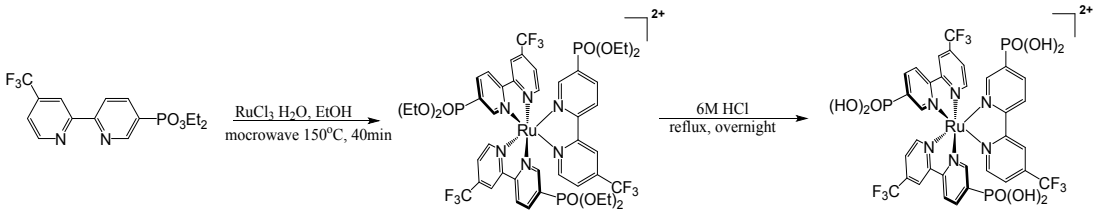

Figure S21. Synthesis of [Ru(4-CF_3-5′-PO_3H_2-bpy)$_3$]Cl_2 chromophore.

Synthesis of [Ru(4′-CF_3-4-PO_3H_2-bpy)$_3$][Cl]$_2$. The complex was prepared by a modification of the procedure reported for [Ru(4,4'-$(PO_3H_2)_2$-bpy)$_3$]Cl_2.[5] $RuCl_3 \cdot 3H_2O$ (61 mg, 0.233 mmol) and diethyl (4′-(trifluoromethyl)-[2,2'-bipyridin]-5-yl)phosphonate (335 mg, 0.93 mmol) were suspended in 40 mL of EtOH. The mixture was heated at 150 °C in a microwave reactor for 4 hours and periodically monitored by UV-vis until only the ^{1}MLCT (~460nm) absorption is present. After removing the solvent and washing the solid with diethyl ether, a mixture of [Ru(4′-CF_3-4-PO_3Et_2-bpy)$_3$]Cl_2 and [Ru(4′-CF_3-4-PO_3H_2-bpy)$_3$]Cl_2 was obtained. The mixture was then hydrolyzed in 6M HCl at 120 °C overnight. After removing the solvent by rotatory evaporation, the material was purified by chromatography on Sephadex LH20 to provide the title complex as an orange-red solid (200 mg, 83% yield). ^{1}H NMR (400 MHz, D_2O): δ 8.48 – 8.36 (m, 2H), 7.61 (dd, J = 10.4, 9.7 Hz, 1H), 7.37 – 7.16 (m, 3H). HR-MS (ESI): m/z^{+} = 504.9728 (M^{2+} - $4H^{+}$). Elemental Analysis (calcd., found) for $C_{33}H_{24}F_9N_6O_9P_3RuCl_2 \cdot 4H_2O$: C (34.27, 33.91), H (2.79, 2.77), N (7.27, 6.95).

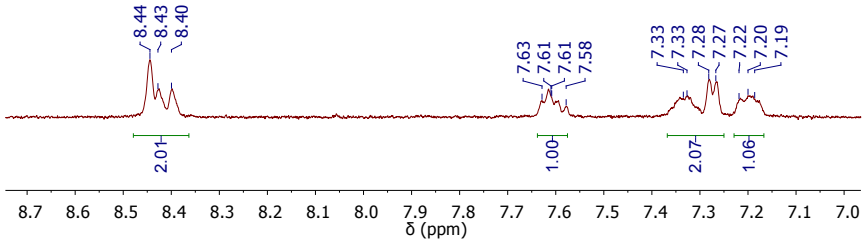

Figure S22. ^{1}H NMR spectrum for [Ru(4′-CF_3-4-PO_3H_2-bpy)$_3$]Cl_2 in D_2O.

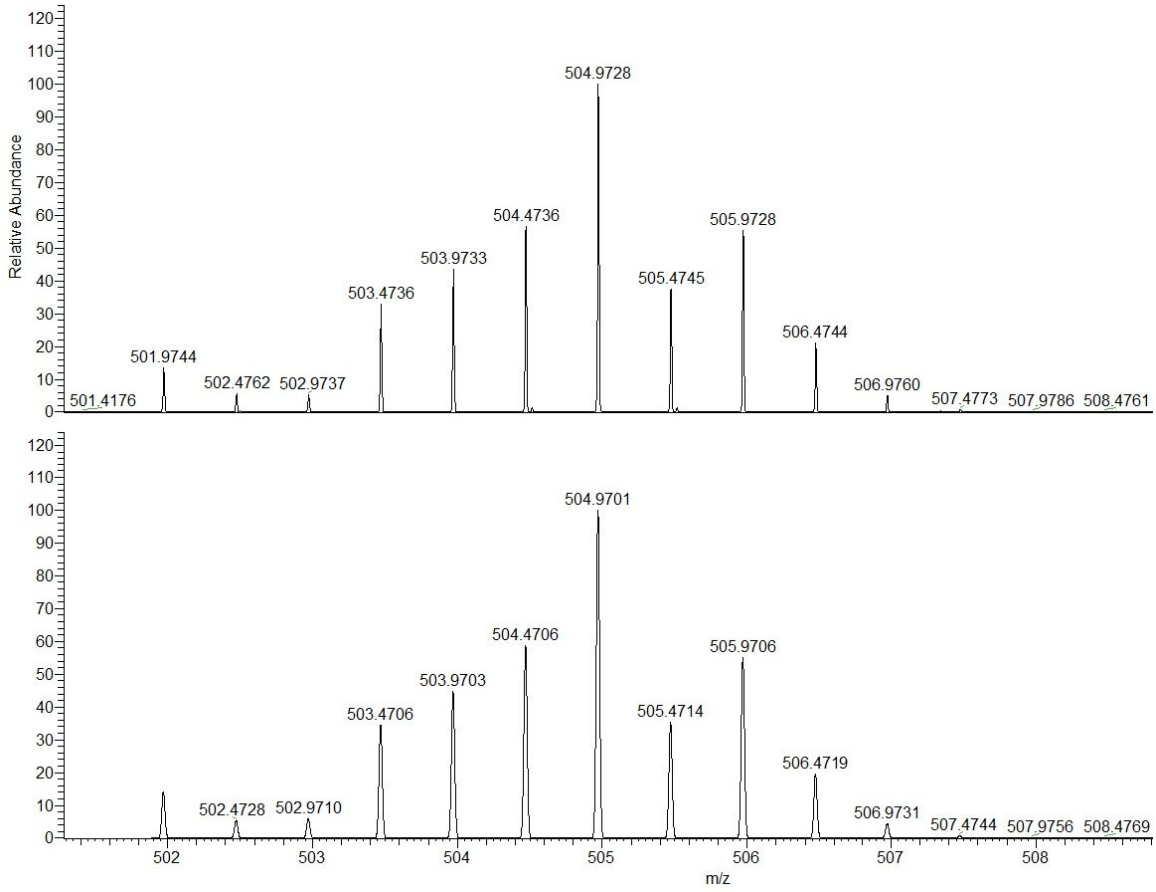

Figure S23. Experimental (top) and simulated (bottom) mass spectrum for [Ru(4′-CF_3-4-PO_3H_2-bpy)$_3$]Cl_2 in MeOH.

Synthesis of [Ru(4′-CF_3-5-PO_3H_2-bpy)$_3$]Cl_2. A procedure similar to **[Ru(4′-CF_3-4-PO_3H_2-bpy)$_3$]Cl_2** was used substituting diethyl (4′-(trifluoromethyl)-[2,2′-bipyridin]-5-yl)phosphonate (335 mg, 0.93 mmol) in place of diethyl (4′-(trifluoromethyl)-[2,2'-bipyridin]-4-yl)phosphonate. Yield: 210 mg, ~85%. ^{1}H NMR (400 MHz, D_2O): δ 8.65 (s, 1H), 8.41 (s, 1H), 8.09 (d, J = 8.8 Hz, 1H), 7.98 – 7.72 (m, 2H), 7.45 (s, 1H). HR-MS (ESI): m/z^{+} = 504.9727 (M^{2+} - 4H^{+}). Elemental

Analysis (calcd., found) for $C_{33}H_{24}F_9N_6O_9P_3RuCl_2 \cdot 4H_2O$: C (34.27, 34.45), H (2.79, 2.82), N (7.27, 6.96).

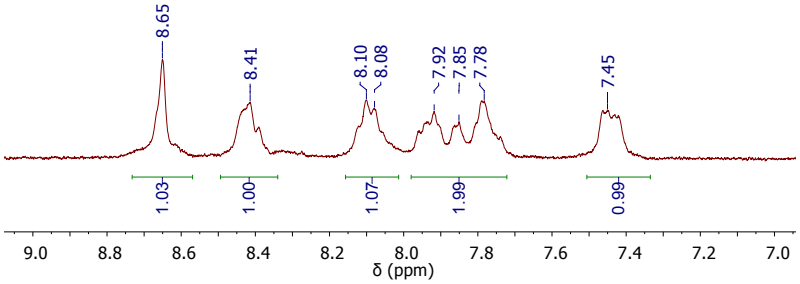

Figure S24. ^{1}H NMR spectrum for $[Ru(4'\text{-}CF_3\text{-}5\text{-}PO_3H_2\text{-}bpy)_3]Cl_2$ in D_2O.

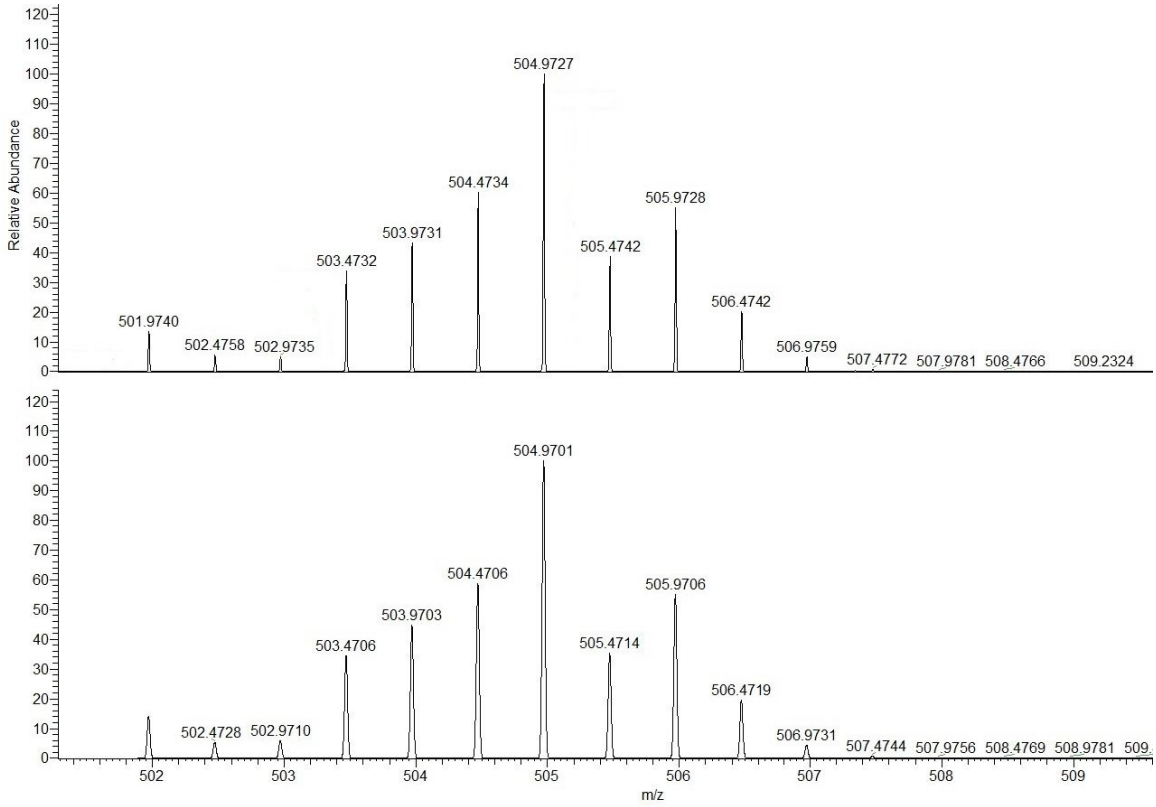

Figure S25. Experimental (top) and simulated (bottom) mass spectrum for $[Ru(4'\text{-}CF_3\text{-}5\text{-}PO_3H_2\text{-}bpy)_3]Cl_2$.

Synthesis of $[Ru(4\text{-}PO_3H_2\text{-}bpy)_3]Cl_2$. $[Ru(4\text{-}PO_3H_2\text{-}bpy)_3]Cl_2$ was synthesized by a procedure similar to $[Ru(4\text{-}CF_3\text{-}5\text{-}PO_3H_2\text{-}bpy)_3]Cl_2$ except that diethyl [2,2′-bipyridin]-4-ylphosphonate (292 mg, 1 mmol) was used in place of diethyl (4′-(trifluoromethyl)-[2,2'-bipyridin]-5-yl)phosphonate and reacted at 150 °C in the microwave for 40 minutes**.** Yield: 165 mg, 80%. ^{1}H NMR (400 MHz,

D_2O): δ 8.31 (dd, J = 11.2, 3.9 Hz, 1H), 8.19 (d, J = 8.1 Hz, 1H), 7.70 (dd, J = 12.0, 7.6 Hz, 1H), 7.52 – 7.28 (m, 2H), 7.23 – 7.10 (m, 1H), 7.01 (d, J = 5.9 Hz, 1H). HR-MS (ESI): m/z$^+$ = 806.9897 (M^{2+} - 3H$^+$). Elemental Analysis (calcd., found) for $C_{30}H_{27}N_6O_9P_3RuCl_2 \cdot H_2O$: C (40.10, 40.13), H (3.25, 3.29), N (9.35, 9.18).

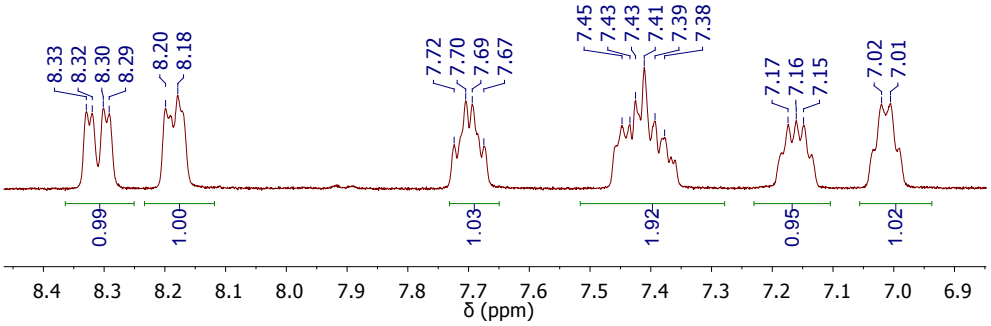

Figure S26. ^{1}H NMR spectrum for [Ru(4-PO_3H_2-bpy)$_3$]Cl_2 in D_2O.

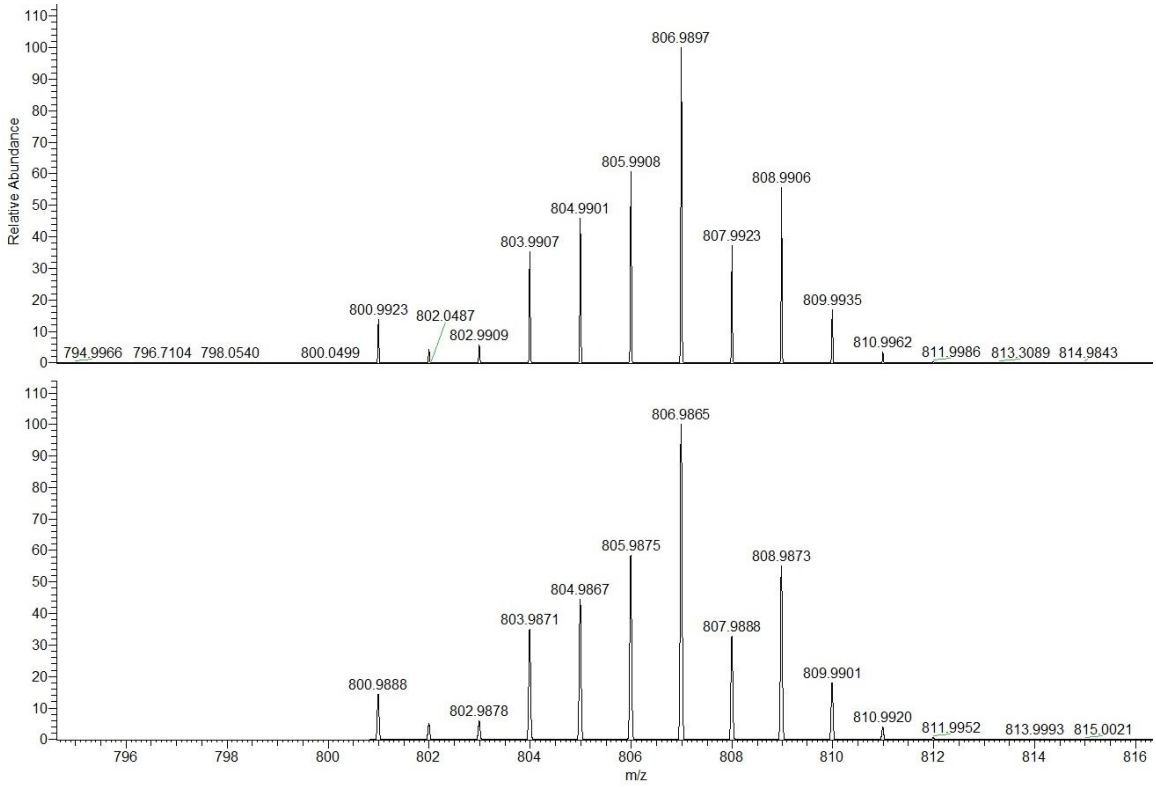

Figure S27. Experimental (top) and simulated (bottom) mass spectrum for [Ru(4-PO_3H_2-bpy)$_3$]Cl_2.

Synthesis of [Ru(5-PO_3H_2-bpy)$_3$]Cl_2. [Ru(5-PO_3H_2-bpy)$_3$]Cl_2 was synthesized by a procedure similar to [Ru(4-PO_3H_2-bpy)$_3$]Cl_2 except that diethyl [2,2′-bipyridin]-5-ylphosphonate (292 mg, 1 mmol) was used in place of diethyl [2,2′-bipyridin]-4-ylphosphonate. Yield: 165 mg, 80%. ^{1}H NMR (400 MHz, D_2O): δ 8.11 (dd, J = 13.4, 6.3 Hz, 2H), 7.79 (t, J = 8.3 Hz, 1H), 7.65 (dt, J = 17.3, 8.1 Hz, 2H), 7.43 – 7.27 (m, 1H), 6.99 – 6.91 (m, 1H). HR-MS (ESI): m/z$^+$ = 806.9908 (M^{2+} - 3H^+). Elemental Analysis (calcd., found) for $C_{30}H_{26}N_6O_9P_3RuCl \cdot H_2O$: C (41.8, 42.07), H (3.27, 3.31), N (9.75, 9.81).

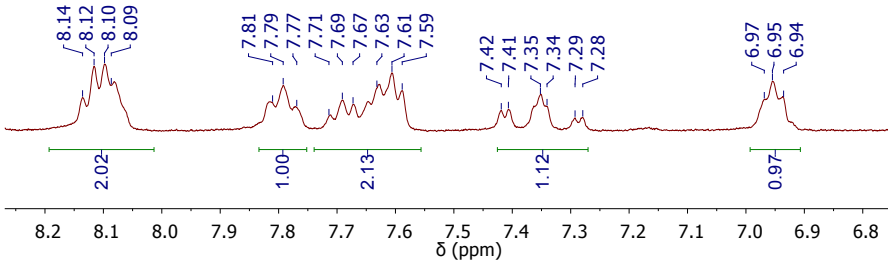

Figure S28. ^{1}H NMR spectrum for [Ru(5-PO_3H_2-bpy)$_3$]Cl_2 in D_2O.

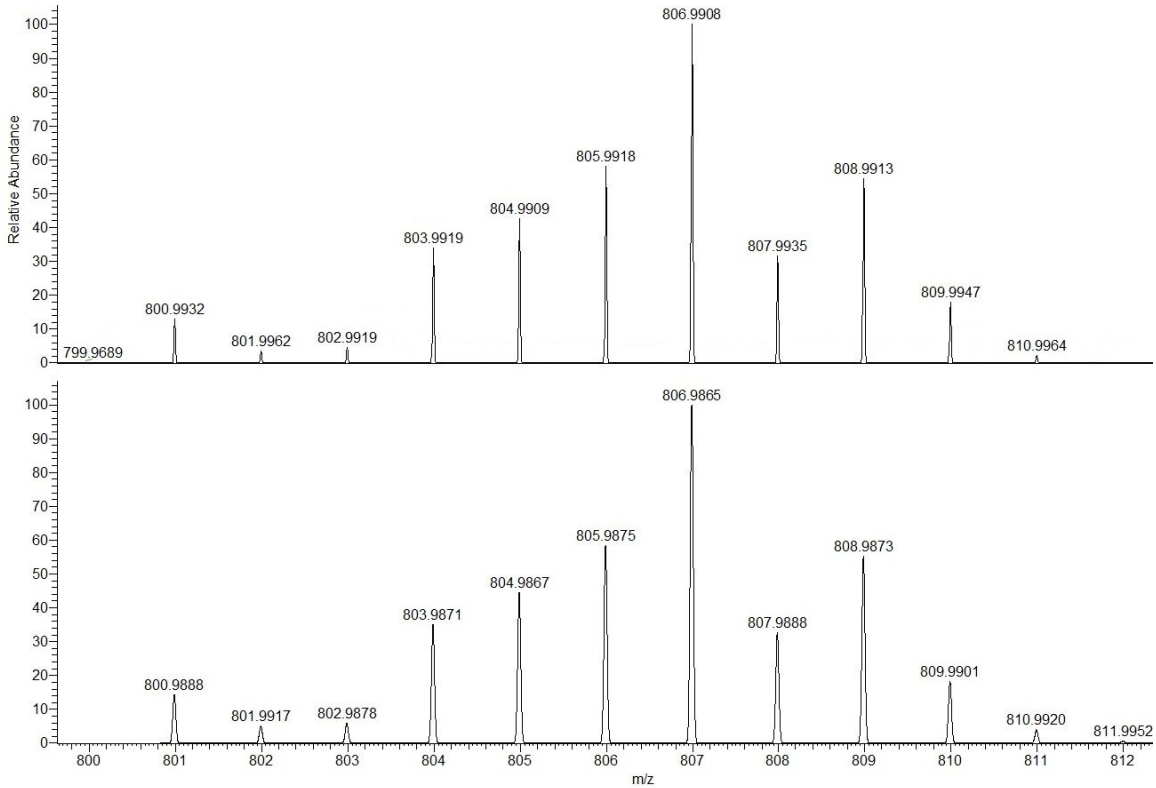

Figure S29. Experimental (top) and simulated (bottom) mass spectrum for [Ru(5-PO_3H_2-bpy)$_3$]Cl_2.

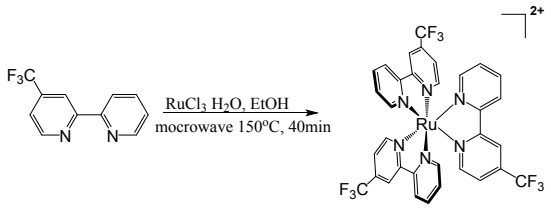

Figure S30. Synthesis of $[Ru(4\text{-}CF_3\text{-}bpy)_3](OTf)_2$ chromophore.

Synthesis of $[Ru(4\text{-}CF_3\text{-}bpy)_3](OTf)_2$. $[Ru(4\text{-}CF_3\text{-}bpy)_3](OTf)_2$ was prepared by a procedure analogous to the other complexes. $RuCl_3 \cdot 3H_2O$ (90 mg, 0.344 mmol) and 4-(trifluoromethyl)-2,2′-bipyridine (350 mg, 1.56 mmol) were suspended in 40 mL EtOH. The mixture was heated at 150 °C in the microwave for 4 hours. After removing the solvent, a saturated aqueous solution of LiOTf was added to precipitate and an orange-red solid, which was collected by filtration. Final purification was achieved by chromatography on silica eluting with acetonitrile and LiOTf. After concentrating the solution to ~5mL, a saturated aqueous solution of LiOTf was added to precipitate again and to obtain the pure product. Yield: 340 mg, 92%. ^{1}H NMR (400 MHz, CD_3CN): δ 8.78 (s, 2H), 8.67 (d, J = 8.2 Hz, 2H), 8.14 (t, J = 7.9 Hz, 2H), 8.00 (d, J = 5.9 Hz, 1H), 7.91 (t, J = 5.5 Hz, 1H), 7.78 (d, J = 5.5 Hz, 1H), 7.71 (t, J = 5.0 Hz, 1H), 7.64 (d, J = 5.9 Hz, 2H), 7.51 – 7.44 (m, 2H). HR-MS (ESI): m/z^+ = 923.0248 (M^{2+} + OTf^-). Elemental Analysis (calcd., found) for $C_{35}H_{21}S_2F_{15}N_6O_6Ru \cdot H_2O$: C (38.36, 38.29), H (1.86, 1.77), N (7.65, 7.62).

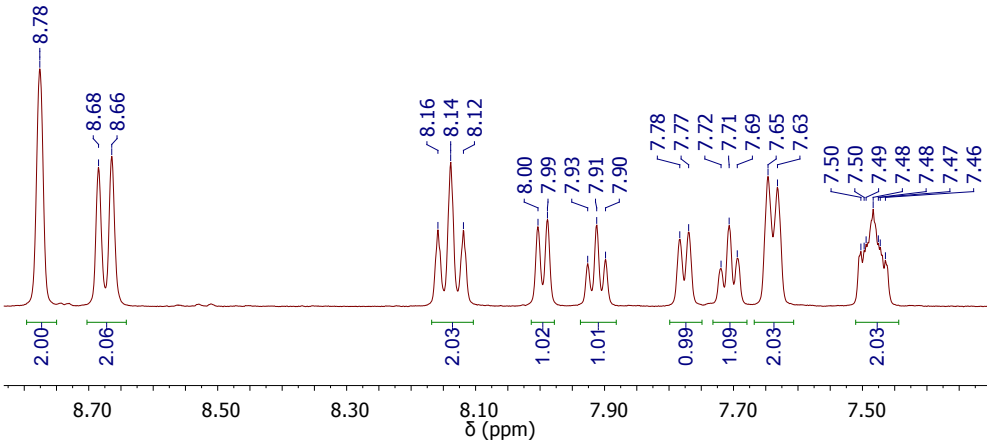

Figure S31. ^{1}H NMR spectrum for $[Ru(4\text{-}CF_3\text{-}bpy)_3](OTf)_2$ in CD_3CN.

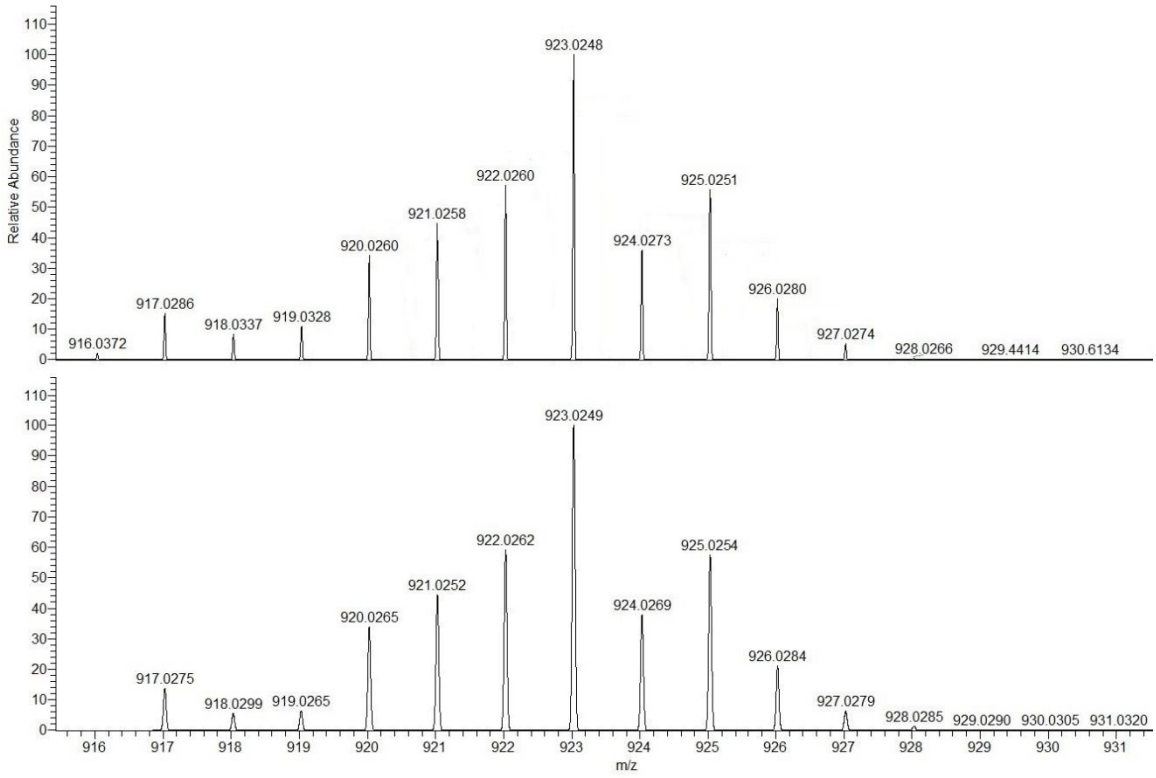

Figure S32. Experimental (top) and simulated (bottom) mass spectrum for [Ru(4-CF_3-bpy)$_3$](OTf)$_2$.

Synthesis of [Ru(5-CF_3-bpy)$_3$](PF$_6$)$_2$. [Ru(5-CF_3-bpy)]$_3$(PF_6)$_2$ was synthesized by a procedure analogous to [Ru(4-CF_3-bpy)$_3$](OTf)$_2$ except that 5-(trifluoromethyl)-2,2′-bipyridine (350 mg, 1.56 mmol) was used in place of 4-(trifluoromethyl)-2,2′-bipyridine and in the final precipitation, NH_4PF_6 was used instead of LiOTf. Yield: 350 mg, 96%. ^{1}H NMR (400 MHz, CD_3CN): δ 8.67 (d, *J* = 8.6 Hz, 1H), 8.60 (d, *J* = 8.1 Hz, 1H), 8.37 (d, *J* = 8.7 Hz, 1H), 8.14 (dd, *J* = 9.7, 6.0 Hz, 1H), 7.98 (s, 1H), 7.87 (d, *J* = 4.4 Hz, 1H), 7.75 (d, *J* = 6.2 Hz, 1H), 7.64 (d, *J* = 5.3 Hz, 1H), 7.52 – 7.44 (m, 1H). HR-MS (ESI): m/z$^+$ = 919.0370 (M $^{2+}$ + PF_6^-). Elemental Analysis (calcd., found) for $C_{33}H_{21}F_{21}N_6P_2Ru$: C (36.84, 36.90), H (1.90, 1.80), N (7.85, 7.88).

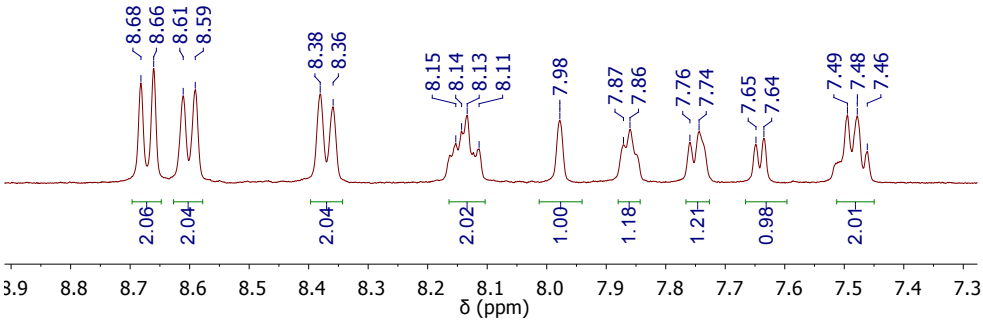

Figure S33. ^{1}H NMR spectrum for $[Ru(5\text{-}CF_3\text{-}bpy)_3](PF_6)_2$ in CD_3CN.

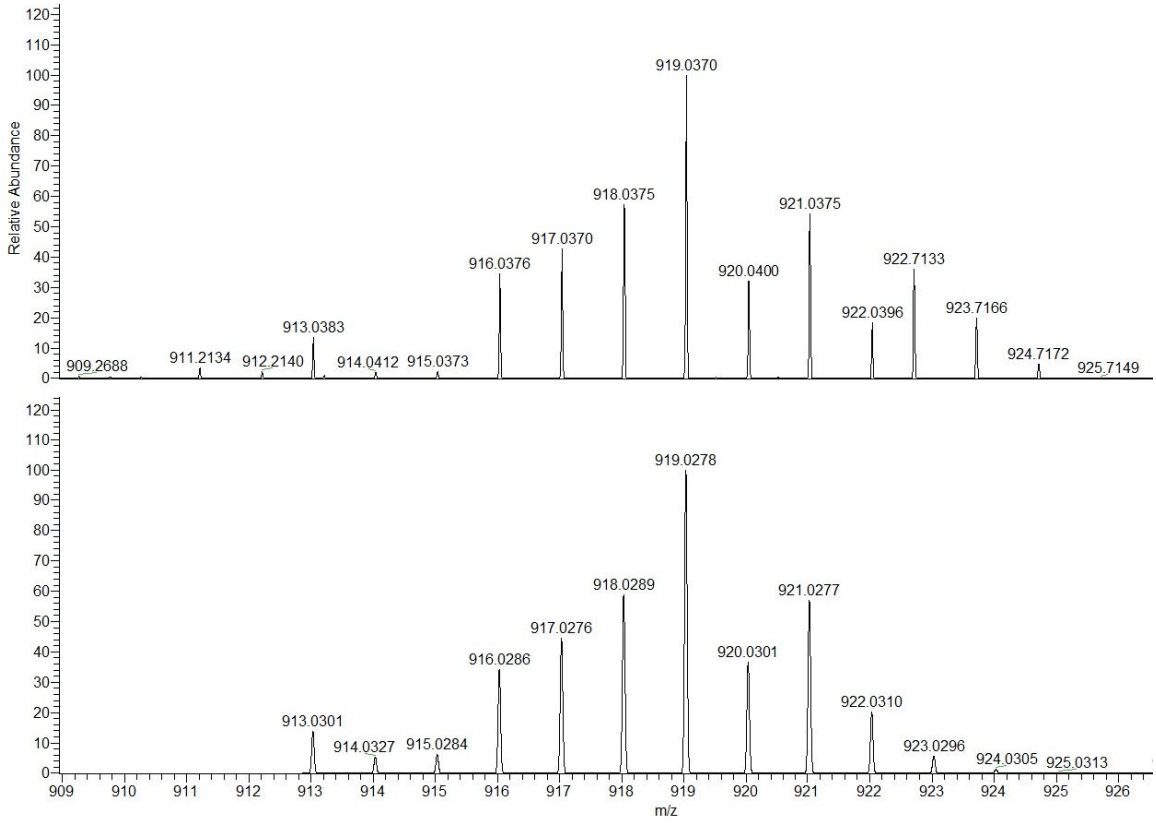

Figure S34. Experimental (top) and simulated (bottom) mass spectrum for $[Ru(5\text{-}CF_3\text{-}bpy)_3](PF_6)_2$.

Synthesis of $[Ru(bpy)_2(5\text{-}PO_3H_2\text{-}bpy)]Cl_2$. $[Ru(bpy)_2(5\text{-}PO_3H_2\text{-}bpy)_3]Cl_2$ was synthesized by a similar procedure to $[Ru(bpy)_2(4,4'\text{-}(PO_3H_2)_2\text{-}bpy)]Cl_2$,[6] starting from $[Ru(bpy)_2Cl_2]$ (113 mg, 0.233 mmol) and diethyl [2,2′-bipyridin]-5-ylphosphonate (68 mg, 0.233 mmol, 1 equiv.) After removing the solvent and washing the solid with diethyl ether, the mixture was hydrolyzed in 6M

HCl at 120 °C overnight. After removing the solvent by rotatory evaporation and purification by chromatography on Sephadex LH20, an orange red solid was obtained. Yield: 125 mg, 75%. ^{1}H NMR (400 MHz, D_2O): δ 7.90 (t, J = 7.4 Hz, 5H), 7.64 – 7.55 (m, 2H), 7.43 (dd, J = 17.8, 7.9 Hz, 6H), 7.20 – 7.04 (m, 5H), 6.83 – 6.66 (m, 5H). HR-MS (ESI): m/z$^+$ = 649.0695 (M^{2+} - H^+). Elemental Analysis (calcd., found) for $C_{30}H_{25}N_6O_3PRuCl_2 \cdot 3HCl$: C (43.42, 43.68), H (3.40, 3.31), N (10.13, 9.86).

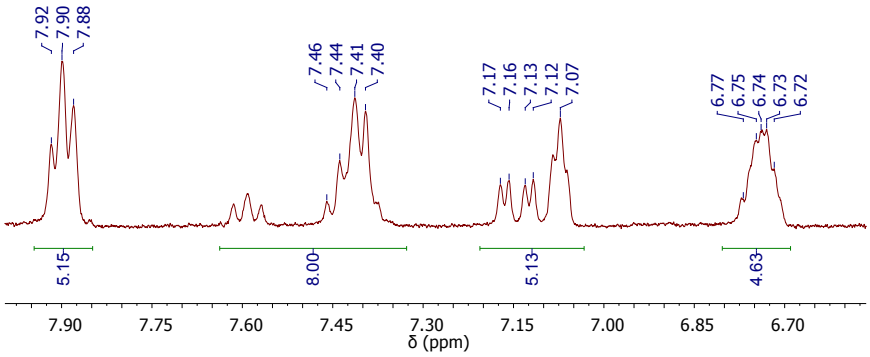

Figure S35. ^{1}H NMR spectrum for $[Ru(bpy)_2(5\text{-}PO_3H_2\text{-}bpy)]Cl_2$ in D_2O.

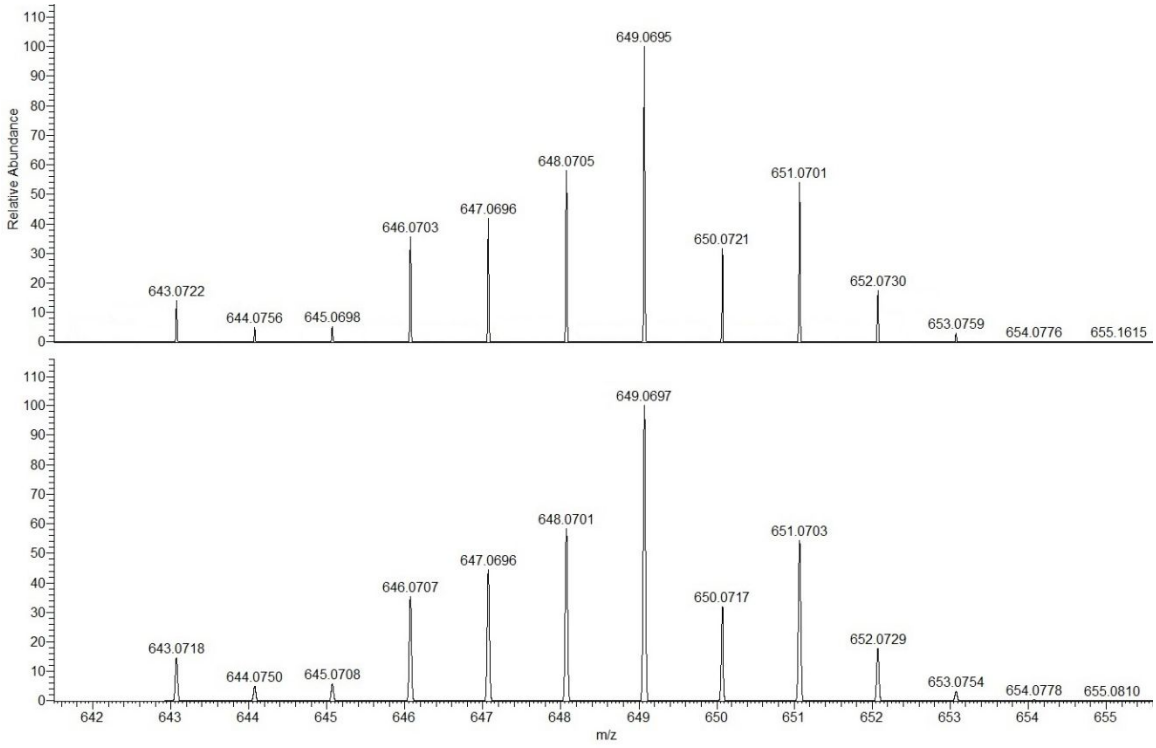

Figure S36. Experimental (top) and simulated (bottom) mass spectrum for $[Ru(bpy)_2(5\text{-}PO_3H_2\text{-}bpy)]Cl_2$.

Synthesis of [Ru(5-Me-5′-CH_2-PO_3H_2-bpy)$_3$]Cl_2. [Ru(5-Me-5′-CH_2-PO_3H_2-bpy)$_3$]Cl_2 was synthesized by a procedure similar to [Ru(4-PO_3H_2-bpy)$_3$]Cl_2 except that diethyl ((5′-methyl-[2,2′-bipyridin]-5-yl)methyl)phosphonate (240 mg, 0.212 mmol) was used in place of diethyl [2,2′-bipyridin]-4-ylphosphonate. Yield: 70% (143 mg). ^{1}H NMR (400 MHz, D_2O): δ 8.13 (s, 2H), 7.53 (dd, *J* = 139.6, 50.8 Hz, 4H), 2.54 (d, *J* = 97.8 Hz, 2H), 1.91 (s, 3H). HR-MS (ESI): m/z$^+$ = 891.0834 (M^{2+} - 3H^+). Elemental Analysis (calcd., found) for $C_{36}H_{39}N_6O_9P_3RuCl_2 \cdot H_2O \cdot 2CH_3OH$: C (43.60, 43.85), H (4.72, 4.77), N (8.03, 8.06).

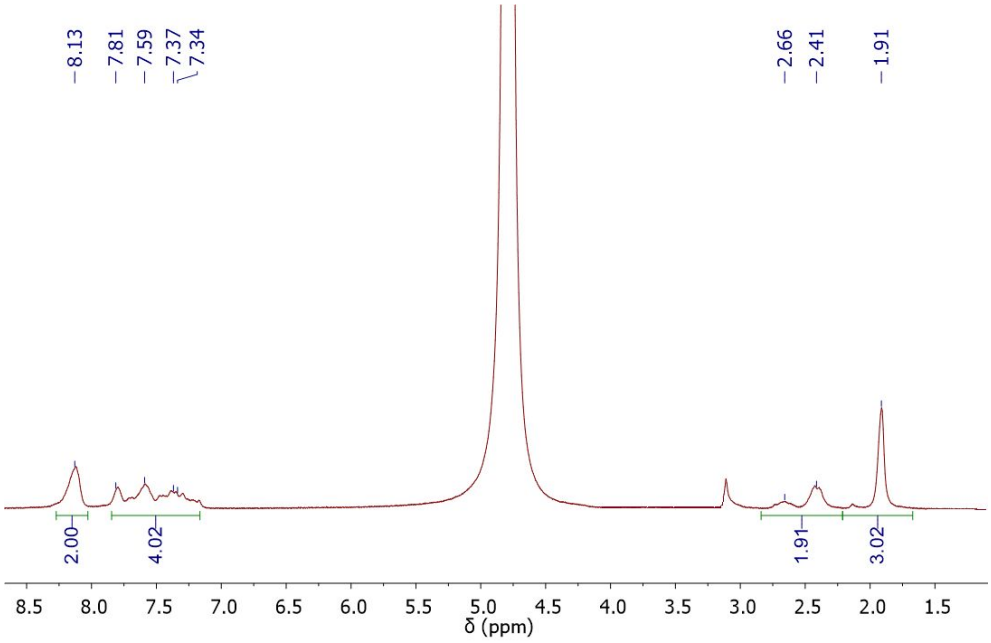

Figure S37. ^{1}H NMR spectrum for [Ru(5-Me-5′-CH_2-PO_3H_2-bpy)$_3$]Cl_2 in D_2O.

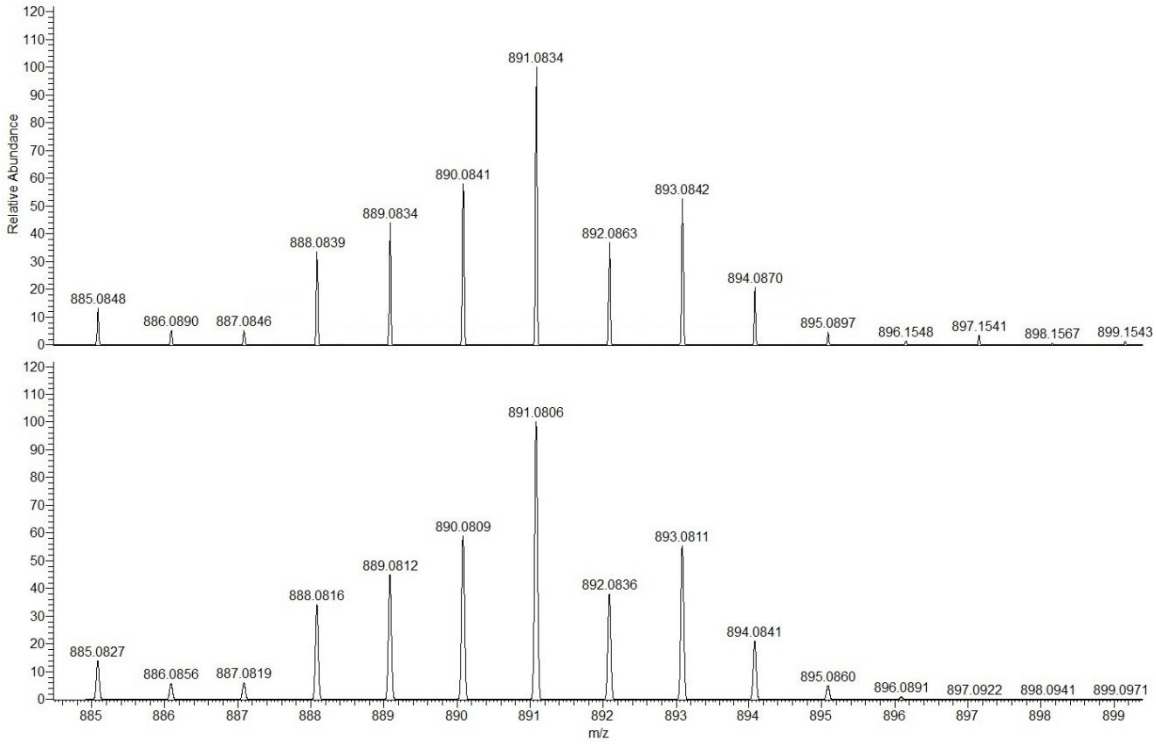

Figure S38. Experimental (top) and simulated (bottom) mass spectrum for [Ru(5-Me-5′-CH_2-PO_3H_2-bpy)$_3$]Cl_2.

References

1. Harris, R. K.; Becker, E. D.; Cabral de Menezes, S. M.; Goodfellow, R.; Granger, P., NMR nomenclature. Nuclear Spin Properties and Conventions for Chemical Shifts (IUPAC Recommendations 2001). *Pure Appl. Chem.* **2001,** *73*, 1795-1818.
2. Juris, A.; Balzani, V.; Barigelletti, F.; Campagna, S.; Belser, P.; von Zelewsky, A., Ru(II) Polypyridine Complexes: Photophysics, Photochemistry, Eletrochemistry, and Chemiluminescence. *Coord. Chem. Rev.* **1988,** *84*, 85-277.
3. Lakowicz, J. R., *Principles of Fluorescence Spectroscopy*. Springer Science & Business Media: 2013.
4. Van Houten, J.; Watts, R. J., Temperature Dependence of the Photophysical and Photochemical Properties of the Tris(2, 2'-bipyridyl)ruthenium (II) Ion in Aqueous Solution. *J. Am. Chem. Soc.* **1976,** *98*, 4853-4858.
5. Shaffer, D. W.; Xie, Y.; Szalda, D. J.; Concepcion, J. J., Manipulating the Rate-Limiting Step in Water Oxidation Catalysis by Ruthenium Bipyridine–Dicarboxylate Complexes. *Inorg. Chem.* **2016,** *55*, 12024-12035.
6. Norris, M. R.; Concepcion, J. J.; Glasson, C. R.; Fang, Z.; Lapides, A. M.; Ashford, D. L.; Templeton, J. L.; Meyer, T. J., Synthesis of Phosphonic Acid Derivatized Bipyridine Ligands and their Ruthenium Complexes. *Inorg. Chem.* **2013,** *52*, 12492-12501.